Asymmetrical 4 × 4 Butler Matrix and its Application for Single Layer 8 × 8 Butler Matrix

Ali Tajik, Ahmad Shafiei Alavijeh, and Mohammad Fakharzadeh, *Senior Member, IEEE*

***Abstract*— The design procedure and measured results of a novel 4 × 4 Butler matrix are presented in this paper. This asymmetrical structure provides fairly flexible phase outputs; therefore, the array radiation pattern can be rotated around the array normal axis. The structure of this modified Butler matrix is discussed in detail, and the explicit design formulas are derived to achieve the arbitrary main beams direction. Using the proposed design procedure, the Butler matrix can provide even broadside and endfire beams. In addition, this structure is employed to design two Butler matrices, which generate similar patterns as a conventional 8 × 8 Butler matrix, using only single layer circuits with significantly lower sizes. Both structures are implemented for Wi-Fi frequency (2.45 GHz), and the measured results are presented. The first structure employs two asymmetrical 4 × 4 Butler matrices, while the second one uses only one 4 × 4 Butler matrix with single-pole double-throw (SPDT) switches added to select the proper constant phase shifts. The measured return loss, the average insertion loss, and the fractional bandwidth for the first structure are ≥23 dB, 6.6 dB, and 24%, respectively. These parameters for the second structure are ≥17 dB, 7.8 dB, and 20%, respectively. Moreover, the size reduction for the first and second structures compared to a conventional 8 × 8 Butler matrix is about 50% and 80%, respectively.**

***Index Terms*— Asymmetrical Butler matrix, beam-forming network (BFN), beam steering, phased array, phase shifter, simplified 8 × 8 Butler matrix, single layer.**

I. Introduction

BUTLER matrix is a low-cost, simple, passive switching beam network, which is frequently used to steer the array beam to certain directions [1]–[4]. Butler matrix has many applications. For example, it is used for satellite applications [5] design of power amplifiers for multiple-input multiple-output (MIMO) systems [6], or to send and receive data between multiple users [7], [8]. However, there is no flexibility in designing the beam direction in the classic structures. Furthermore, the conventional higher order Butler matrices, such as 8 × 8 use multilayer structures with several passive components, which result in high insertion loss, large structure size, high sidelobe level, and low beam crossing levels (BCLs) or large ripples in the total array coverage function.

Manuscript received October 27, 2018; revised January 31, 2019; accepted April 7, 2019. Date of publication May 20, 2019; date of current version August 12, 2019. *(Corresponding author: Mohammad Fakharzadeh.)*

The authors are with the Electrical Engineering Department, Sharif University of Technology, Tehran 14588-89694, Iran (e-mail: ali.tajik92@yahoo.com; ahmadshafiei_a@yahoo.com; fakharzadeh@sharif.edu).

Color versions of one or more of the figures in this paper are available online at http://ieeexplore.ieee.org.

Digital Object Identifier 10.1109/TAP.2019.2916695

Innovations in the Butler matrix design can be categorized into three major classes. Being a passive structure, consisting of quarter-wavelength couplers and crossovers, the physical size of the conventional Butler matrices is relatively large. Thus, many authors have worked on reducing the effective size of the structure [9]–[11]. The second class of designs focuses on the bandwidth improvement of the structure [9], [12]. The last class addresses the reduction of the sidelobe level of the beam pattern [13], [14].

Most of the previous works report on the modifications of the 4 × 4 Butler matrix, which switches the array beam between four symmetrical directions. Higher order Butler matrices, such as 8 × 8, become impractically large in size, due to a large number of couplers and crossovers; thus, they are rarely reported. Nevertheless, a multilayer implementation of 8 × 8 Butler matrix is presented in [15]. Also, in [16], the 8 × 8 structure is realized in CMOS technology. Both cases have a noticeable cost compared to a single layer microstrip realization.

Very recently, new structures for the Butler matrix with flexible output phase differences are demonstrated in [17] and [18]. For example, Ren *et al.* [17] employ flexible couplers instead of the conventional branch line coupler (BLC). Although this is a novel structure with a wide range of output phase from −180° to 180°, designing a coupler with arbitrary phase response and equal output power is a complicated task. Furthermore, in [18] phase reconfigurable synthesized transmission lines are used at the outputs of a standard Butler matrix to directly change the output phases similar to a phase shifter, which increases the complexity and power consumption compared to the pure passive microwave structures.

This paper proposes a general structure for the Butler matrix, which employs conventional BLCs and more constant phase shift sections to generate any progressive phase difference (PPD) from −180° to 180°. This is different from the conventional Butler matrix, which has just ±45° or ±135° PPDs between the output elements. The proposed structure is robust and simple since it can be realized in a single layer, low-cost PCB.

The ability to design endfire and broadside beams is one of the interesting applications of this structure, which overcomes one of the main defects of the conventional Butler matrices. An important application that can be implemented by this structure is constructing an 8 × 8 Butler matrix in single layer PCB as well as monolithic integrated circuits. Two structures, which use this idea are presented in Section III, which have a

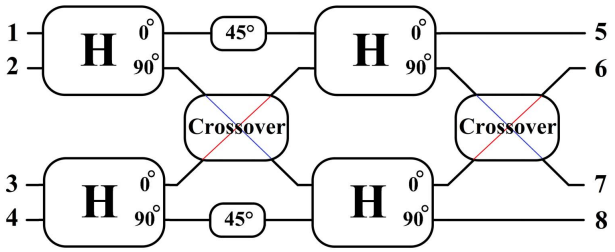

Fig. 1. Structure of the conventional 4 × 4 Butler matrix.

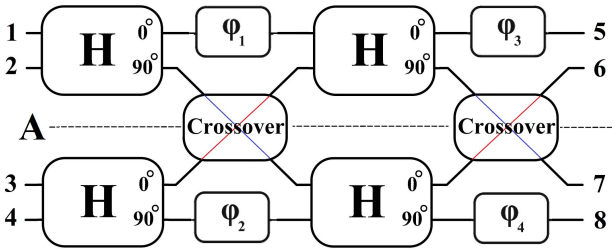

Fig. 2. Structure of the asymmetrical 4 × 4 Butler matrix.

similar pattern as a conventional 8 × 8 Butler matrix, but with a size reduction of nearly 80%. These structures are fabricated, and the results of simulation and measurements are presented in Section IV. The simulated beam patterns of these structures are very smooth with less than 1 dB ripple against conventional 8 × 8 Butler matrices, where the crossing level of the adjacent beams is 3 dB lower than the peak gain.

II. Modified Butler Matrix

In this section, first, the structure of a conventional 4 × 4 Butler matrix is discussed. Then, a novel structure based on modifying the conventional Butler matrix is explained. It is shown how the proposed structure overcomes the conventional Butler matrix shortcoming to provide an arbitrary main direction.

A. Conventional 4 × 4 Butler Matrix

Fig. 1 shows a conventional Butler matrix structure, with four input ports named from ports 1–4, and four output ports, denoted by ports 5–8; thus, it is called a 4 × 4 Butler matrix. The outputs of the matrix could feed a line of antennas to form a linear array of four antennas. By exciting any input port on the left side of the matrix, four outputs with equal power but different phases are generated. The sequenced ports have identical phase differences, called PPD (i.e., output phases are $\alpha, \alpha+\beta, \alpha+2\beta, \alpha+3\beta$, where β is named PPD). Based on the array antenna theory, by applying these phases, the main beam in a particular angle is formed [19]. Thus, this structure generates four main beams corresponding to the excited input port. The conventional Butler matrix shown in Fig. 1 consists of four 90° hybrid couplers, two crossovers, and two constant 45° phase shifts (delay line). By exciting ports 1–4, the PPD values between outputs equal to −45°, 135°, −135°, and 45°, respectively.

The only degree of freedom to change the PPD, which is required to change the beam direction, is to modify the constant phase shift values. Denoting the phase shift value by φ, when the first port is excited, the output phases for ports 5–8 would be $-\varphi$, $-90°$, $-\varphi-90°$, and $-180°$, respectively. The phases are achieved by considering the 0° phase lag for the direct path of 90° hybrid and crossover and −90° for the coupled path of the coupler. To have an identical phase difference for the sequenced ports, (1) must be satisfied

$$\angle S_{61} - \angle S_{51} = \angle S_{71} - \angle S_{61}. \tag{1}$$

TABLE I

Output Phases of the Asymmetrical Butler Matrix for Exciting Different Input Ports

	P1	P2	P3	P4
P5	$-\varphi_1-\varphi_3$	$-90-\varphi_1-\varphi_3$	$-90-\varphi_3$	$-180-\varphi_3$
P6	-90	0	$-180-\varphi_2$	$-90-\varphi_2$
P7	$-\varphi_1-90$	$-180-\varphi_1$	0	-90
P8	$-\varphi_4-180$	$-90-\varphi_4$	$-90-\varphi_2-\varphi_4$	$-\varphi_2-\varphi_4$
PPD	$-45-\frac{\varphi_4}{2}$	$135-\frac{\varphi_4}{2}$	$-135-\frac{\varphi_4}{2}$	$45-\frac{\varphi_4}{2}$
Butler	-45	135	-135	45

Therefore,

$$90-\varphi=\varphi+90-90\rightarrow\varphi=45°. \tag{2}$$

Hence, the only possible value for φ is 45°, which results in a PPD equal to −45° for the first port. By repeating the same procedure for other input ports, it could be deduced that this structure can only generate PPD values of ±45° and ±135°, not any other value between −180° and 180°. Thus, the four beam directions are fixed.

B. Asymmetrical 4 × 4 Butler Matrix

It is possible to add more variables to (2) by employing more constant phase shifts, which results in a modified structure for the Butler matrix that is presented in Fig. 2. Instead of two equal constant phase shifts as in the conventional Butler matrix, there are four unequal constant phase shifts used in the proposed structure, which are denoted by φ_1–φ_4. Table I shows the general output phases of the modified Butler matrix, when each input port is excited.

To achieve the PPD between the outputs when port 1 is excited, (1) must be satisfied. By substituting the values from Table I in (1), we have

$$90-\varphi_1-\varphi_3=\varphi_1+90-90\rightarrow 2\varphi_1+\varphi_3=90. \tag{3}$$

Similarly, the output phases of ports 6–8 are related as

$$\angle S_{71} - \angle S_{61} = \angle S_{81} - \angle S_{71} \tag{4}$$

which gives

$$\varphi_1+90-90=\varphi_4+180-\varphi_1-90\rightarrow 2\varphi_1-\varphi_4=90. \tag{5}$$

Similarly, when port 4 is excited, we conclude

$$\angle S_{64} - \angle S_{54} = \angle S_{74} - \angle S_{64} \tag{6}$$

$$90+\varphi_2-180-\varphi_3=90-90-\varphi_2\rightarrow 2\varphi_2-\varphi_3=90. \tag{7}$$

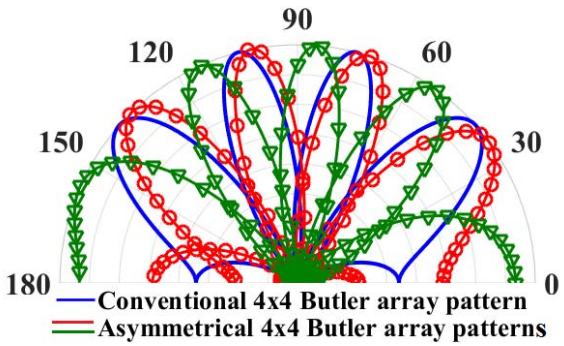

Fig. 3. Comparison of the radiation patterns of the conventional 4×4 Butler matrix (plain blue line) and two asymmetrical 4×4 Butler matrices with $\varphi_4 = 20°$ (red line with circle markers) and $\varphi_4 = -40°$ (green line with triangle markers) for half-wavelength antenna spacing.

It can be shown that extending the same procedure to the other ports does not result in a new relation. By using (3), (5), and (7), after some mathematical simplifications, φ_1, φ_2, and φ_3 can be expressed in terms of φ_4, or

$$\varphi_1 = \frac{90 + \varphi_4}{2}, \quad \varphi_2 = \frac{90 - \varphi_4}{2}, \quad \varphi_3 = -\varphi_4 \tag{8}$$

which implies that the phase shift values are dependent. By employing the values from (8), PPD values are extracted, which are shown in Row 5 of Table I.

It is seen that for $\varphi_4 \neq 0$, the PPDs are different from that of the conventional 4×4 Butler matrix. Indeed, the whole beam patterns of the new modified Butler matrix are rotated relative to the array normal (shown by the dashed line A in Fig. 2), resulting in asymmetrical beams. The conventional Butler matrix is a special case of the new structure, where $\varphi_4 = 0$. Fig. 3 shows the radiation patterns of the conventional Butler matrix and the new structure for two different values of $\varphi_4 = 20°$ and $\varphi_4 = -40°$, which give PPD values for outputs equal to $-55°$, $125°$, $-145°$, and $35°$ for $\varphi_4 = 20°$, and $-25°$, $155°$, $-115°$, and $65°$ for $\varphi_4 = -40°$ according to Table I. Radiation elements are assumed isotropic antennas. The new structure has the potential of covering four directions between $-180°$ and $180°$, which can be determined by choosing the right value for φ_4. Because of the asymmetry of the beam patterns around the array normal, this structure is named *asymmetrical Butler matrix*.

C. Broadside and Endfire Beams

As it is shown in Fig. 3, the conventional 4×4 Butler matrix cannot cover the broadside or endfire directions. But by employing proper phase shifts, it is possible to generate both broadside and endfire beams in an asymmetrical Butler matrix. Fig. 4 shows the beams of an asymmetrical 4×4 Butler matrix with $\varphi_4 = 90°$. In this case, the output ports have the PPD of $\pm 90°$, $0°$, and $180°$. The values of the constant phase shifts, φ_1–φ_4, are presented in (9). The corresponding radiation patterns are displayed in Fig. 4

$$\varphi_1 = 90°, \quad \varphi_2 = 0°, \quad \varphi_3 = -90°, \quad \varphi_4 = 90°. \tag{9}$$

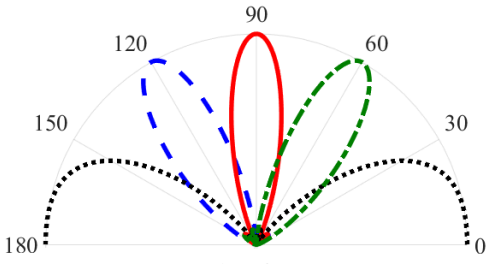

Fig. 4. Broadside and endfire beams, generated by the asymmetrical Butler matrix, considering isotropic antenna elements.

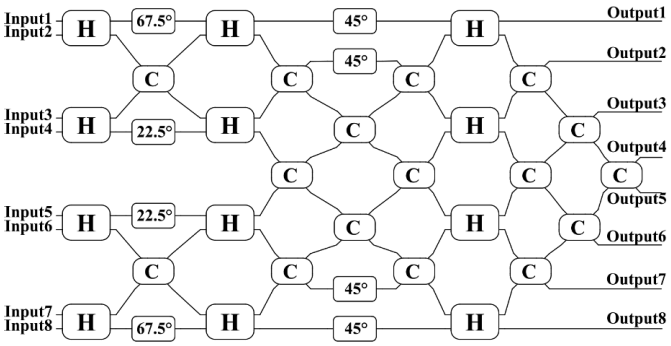

Fig. 5. Conventional 8×8 Butler matrix structure (H: 90° Hybrid, C: crossover).

III. Design of Simplified 8×8 Butler Matrix

The proposed asymmetrical 4×4 Butler matrix can be used as a building block to generate the beam directions of higher order Butler matrices, particularly 8×8 ones. In this section, first, the structure of a conventional 8×8 Butler matrix is investigated. Next, the asymmetrical 4×4 Butler matrix is extended to design a simplified 8×8 Butler matrix. While preserving the properties of the radiation patterns of a conventional 8×8 Butler matrix, the size of this new matrix is much smaller, and the spatial coverage is enhanced.

A. Conventional 8×8 Butler Matrix

The general 8×8 Butler matrix configuration is shown in Fig. 5 [16]. Similar to the 4×4 Butler matrix, by exciting the input ports, this structure generates different PPD values for the outputs, which are equal to $-22.5°$, $157.5°$, $-112.5°$, $67.5°$, $-67.5°$, $112.5°$, $-157.5°$, and $22.5°$. These phases can be divided into two groups.

1) First group: $-67.5°$, $112.5°$, $-157.5°$, and $22.5°$.
2) Second group: $-22.5°$, $157.5°$, $-112.5°$, and $67.5°$.

Considering (8) and Table I, it is concluded that these two groups can be implemented by two asymmetrical Butler matrices with $\varphi_{4,1} = 45°$ and $\varphi_{4,2} = -45°$, respectively. Fig. 6 illustrates the concept of reconstructing the 8×8 Butler matrix beams by starting from conventional 4×4, then rotating the beam axis using two asymmetrical matrices and finally, combining them to achieve the proper pattern.

It should be noted that fabrication of 8×8 Butler matrix is more complicated than a 4×4 one. Moreover, the number of

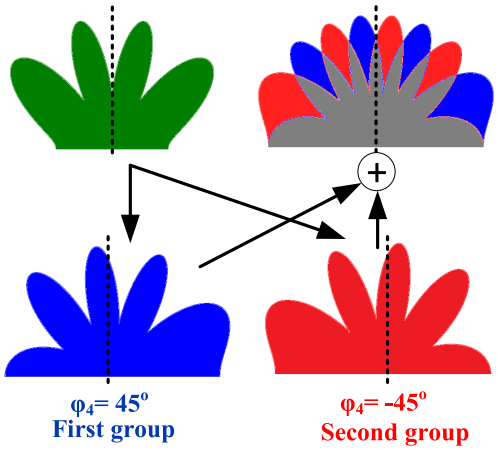

Fig. 6. Concept of designing 8 × 8 Butler matrix using asymmetrical Butler matrix. Dashed line in each figure shows the axis of symmetry of the pattern ($\theta = 90°$).

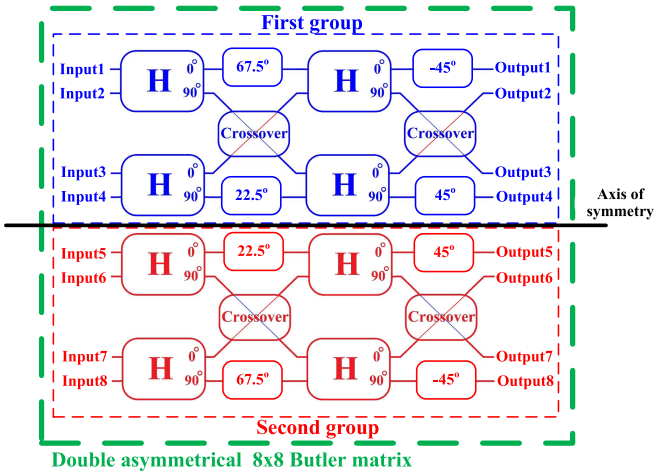

Fig. 7. Structure of double asymmetrical 8 × 8 Butler matrix.

TABLE II
PHASE SHIFTS FOR IMPLEMENTING 8 × 8 BUTLER MATRIX

	φ_4	φ_3	φ_2	φ_1
First group	45°	−45°	22.5°	67.5°
Second group	−45°	45°	67.5°	22.5°

hybrid couplers, crossovers, and phase shifts are 12, 16, and 8, respectively, which make the size of the structure extremely large compared to a 4 × 4 Butler matrix. Consequently, the insertion loss is significantly increased compared to a 4 × 4 one. Considering these drawbacks and the ability to provide the beams of 8 × 8 Butler matrix by employing two asymmetrical Butler matrices, two different architectures for the simplified 8 × 8 Butler matrix are presented hereinbelow. These two structures can provide eight main beams with the same directions as the conventional 8 × 8 Butler matrix.

B. Use of Two Adjacent Asymmetrical 4 × 4 *Butler Matrices*

The first solution is to use two asymmetrical 4 × 4 Butler matrices beside each other. This structure, called double 8 × 8 *asymmetrical Butler matrix*, is shown in Fig. 7. The motivation

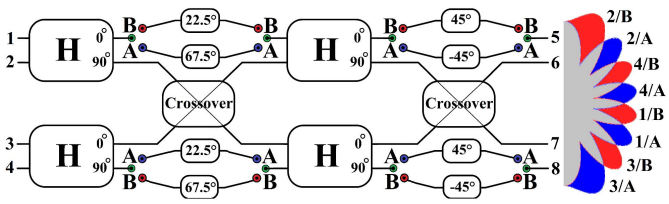

Fig. 8. Structure of the switched version of 8 × 8 Butler matrix.

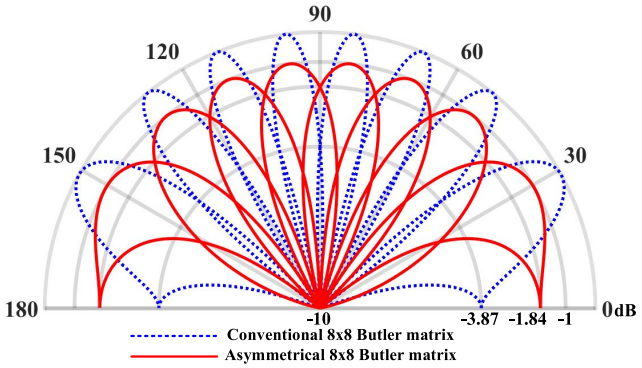

Fig. 9. Comparison of the beams of the conventional 8 × 8 Butler matrix and asymmetrical 8 × 8 Butler matrices.

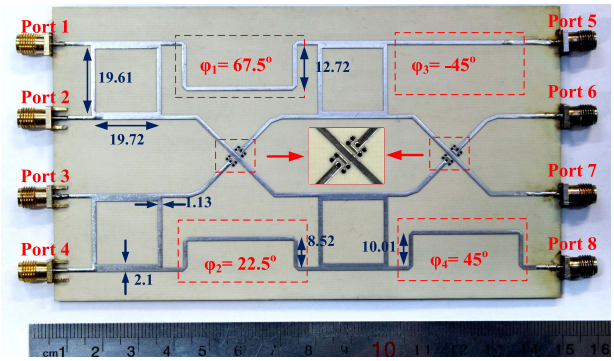

Fig. 10. Fabricated structure of the upper half of the double asymmetrical 8 × 8 Butler matrix. All mentioned lengths are in millimeters.

for this technique originates from Table II, which shows the two phase shifts groups have similarities. In fact, the second group is achieved by flipping the first group around the axis of symmetry, which is shown in Fig. 7. It means that the values of φ_1 and φ_3 of the second structure are equal to φ_2 and φ_4 of the first one. So, both structures are similar except the place of the phase shifts; thus, the time required for designing, simulating, and fabricating is significantly decreased.

C. Use of Switched Asymmetrical Butler Matrix

Since the two structures in Section III-B are similar except for the phase shift values, it is possible to merge them as one structure using RF switches, which choose the right phase shift for each beam direction. This structure is shown in Fig. 8. When the switches are in (A) position, the PPDs of the first group, introduced in Section III-A, are provided. Similarly, the state (B) of the switches, provides the PPDs of the second group.

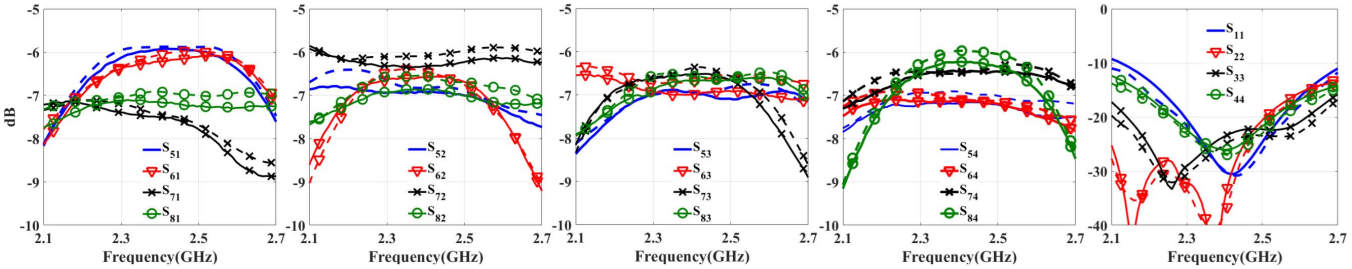

Fig. 11. Simulated (dashed lines) and measured (solid lines) S-parameters of the double asymmetrical 8 × 8 Butler matrix.

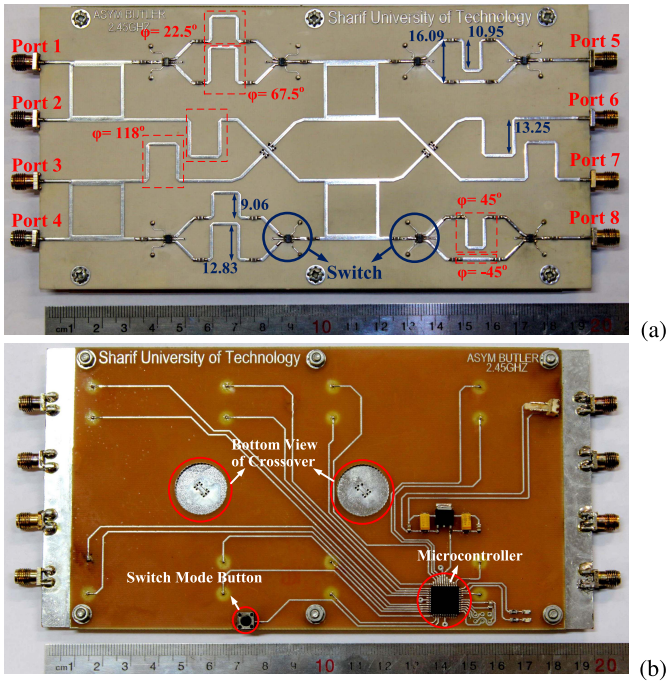

Fig. 12. (a) Fabricated structure of the switched version of the simplified 8 × 8 Butler matrix. All dimensions are in millimeters. (b) Control board.

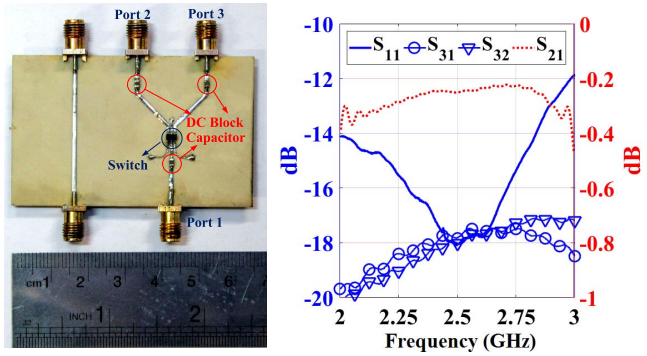

Fig. 13. (a) SPDT switch evaluation board. (b) Measured S-parameters of the switch when the path of ports 1 and 2 is chosen.

TABLE III

SIMULATED AND MEASURED INSERTION LOSS (DECIBEL) OF THE ASYMMETRICAL BUTLER MATRIX

	Simulation				Measurement			
	P1	P2	P3	P4	P1	P2	P3	P4
P5	5.88	6.81	6.93	6.98	5.93	6.95	7.03	7.16
P6	5.98	6.57	6.61	7.12	6.16	6.57	6.93	7.13
P7	7.52	6.04	6.41	6.44	7.58	6.29	6.53	6.45
P8	6.97	6.67	6.62	5.99	7.20	6.90	6.66	6.25

D. Comparison of 8 × 8 *Butler Matrix Structures*

The radiation patterns of the proposed structures are shown in Fig. 9, which are identical. Moreover, the radiation patterns of the conventional 8 × 8 Butler matrix are depicted as well. All feed structures are connected to the isotropic antenna elements. These patterns are drawn by considering a reasonable insertion loss for all blocks. The loss of a 90° hybrid coupler and a crossover are assumed to be 0.5 dB, which is a typical value in the low microwave frequencies. Two points are important, considering the conventional 8 × 8 Butler matrix. First, each signal experiences almost three couplers and four crossovers from its input to the corresponding output, which causes near 3.5 dB loss. For the proposed asymmetrical structures this value is only 1.5 dB (two couplers and one crossover). Second, the imbalance between the outputs of the conventional 8 × 8 Butler matrix is much more than the asymmetrical matrix. For example, in the conventional 8 × 8 Butler, the signal from input 1 to output 1, shown in Fig. 5, experiences just three couplers, which has the loss of 1.5 dB approximately, whereas the signal traveling from input 1 to output 4, propagates through three couplers and seven crossovers, and thus, its insertion loss is nearly 5 dB. This inequality between the output levels can change the beam shape for each direction, particularly degrades the sidelobe levels. Nevertheless, the imbalance between the outputs is only 1 dB for the two asymmetrical structures in the worst situation.

To compare the spatial beam coverage of two structures, the adjacent BCL is used as a figure of merit. In the conventional 8 × 8 Butler, BCL is about 3 dB less than the main lobe peak gain, while this difference is only 1 dB for the asymmetrical 4 × 4 Butler in an ideal lossless structure. So when beams are switched, a more uniform spatial coverage is achieved by the proposed structures. In other words, all users in different directions with the same distance from the antenna, receive almost an equal power level. Noticing the introduced points, Fig. 9 shows that by considering the loss of structures, the gain of the conventional 8 × 8 Butler is about 1 dB greater than the asymmetrical matrices. The difference between the maximum gain of the main beam and the BCL for conventional and asymmetrical structures are 4 and 0.86 dB,

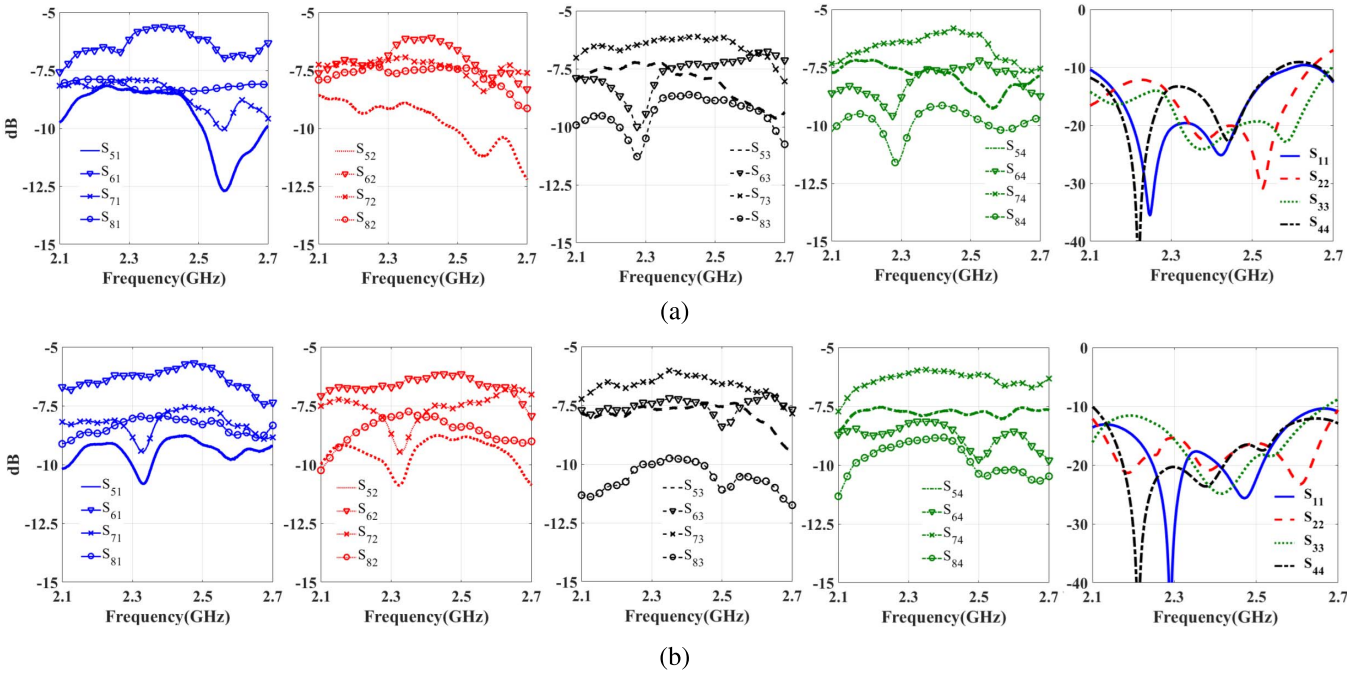

Fig. 14. S-parameters of the switched version of asymmetrical 8 × 8 Butler matrix when the switches are in (a) mode (A) and (b) mode (B).

TABLE IV
SIMULATED AND MEASURED OUTPUT PHASES (DEGREE) OF THE DOUBLE ASYMMETRICAL 8 × 8 BUTLER MATRIX

	Port 1			Port 2			Port 3			Port 4		
	Simulated	Measured	Ideal	Simulated	Measured	Ideal	Simulated	Measured	Ideal	Simulated	Measured	Ideal
Port 5	0	0	0	0	0	0	0	0	0	0	0	0
Port 6	-64.5	-66.2	-67.5	111.8	108.9	112.5	-164.9	-166.9	-157.5	23.4	24.1	22.5
Port 7	-131.7	-131.6	-135	222.5	221.1	225	-316.8	-317.5	-315	47.3	48	45
Port 8	-197.2	-199.6	-202.5	341	336	337.5	-470.2	-470.3	-472.5	65.2	64.1	67.5
PPD			-67.5			112.5			-157.5			22.5

respectively, so BCL in asymmetrical structures is about 2 dB better than the conventional matrix, which shows the capability of uniform spatial coverage in asymmetrical structures.

According to Figs. 5, 7, and 8, the geometry of the asymmetrical Butler matrices is much simpler than the conventional 8 × 8 one. In fact, 8 × 8 Butler contains 12 couplers, 16 crossovers, and 8 phase shift sections. But the double asymmetrical 8 × 8 Butler and switched version of the asymmetrical 8 × 8 Butler have eight and four couplers, and four and two crossovers and eight phase shifts, respectively, with the size reduction near to 60% and 80% compared to the conventional 8 × 8 Butler, considering the length and width of the coupler and crossover about quarter of wavelength. Also, the switched version of 8 × 8 Butler needs just four antennas, with the price of using eight single-pole double-throw (SPDT) switches, while the two other structures need eight antennas. In this case, the reduction in array factor gain in the link budget is almost compensated by the improvement in the Butler matrix insertion loss.

IV. EXPERIMENTAL RESULTS

The two structures introduced in Sections III-B and III-C are fabricated, measured, and compared with the simulation results in this section.

TABLE V
MEASURED INSERTION LOSS (DECIBEL) OF THE SWITCHED VERSION OF ASYMMETRICAL 8 × 8 BUTLER MATRIX

	Mode A				Mode B			
	P1	P2	P3	P4	P1	P2	P3	P4
P5	8.59	9.7	7.86	7.81	8.78	8.79	7.43	7.79
P6	5.67	6.23	7.28	7.52	5.73	6.18	7.47	8.9
P7	8.52	7.28	6.12	5.83	7.56	7.51	6.3	6.18
P8	8.38	7.36	8.66	9.26	8.09	8.16	10.07	9.34

A. Asymmetrical 8 × 8 Butler Matrix

Due to the symmetry in Fig. 7, the upper half of this 8 × 8 Butler matrix was fabricated, which is shown in Fig. 10. This circuit provides the phase shifts values that correspond to the first group given in Table II. This structure is designed for the Wi-Fi frequency (2.45 GHz) on RO4003 substrate with 20 mil thickness and $\epsilon_r = 3.55$. The crossover used in this design is a wideband CPW crossover, which we have presented in [20].

Simulated and measured S-parameters are shown in Fig. 11, where the first four figures show the output S-parameters, and the last one shows the input reflection coefficient. In an ideal case, the S-parameters of the first four figures should

TABLE VI
MEASURED OUTPUT PHASES (DEGREE) OF THE SWITCHED VERSION OF ASYMMETRICAL 8 × 8 BUTLER MATRIX IN BOTH (A) AND (B) MODES

	Mode A								Mode B							
	Port 1		Port 2		Port 3		Port 4		Port 1		Port 2		Port 3		Port 4	
	Measured	Ideal	Measured	Ideal	Measured	Ideal	Measured	Ideal	Measured	Ideal	Measured	Ideal	Measured	Ideal	Measured	Ideal
Port 5	0	0	0	0	0	0	0	0	0	0	0	0	0	0	0	0
Port 6	-74.1	-67.5	99.9	112.5	-159.1	-157.5	23.1	22.5	-25.3	-22.5	149.7	157.5	-115.8	-112.5	66.6	67.5
Port 7	-135.4	-135	219	225	-319.1	-315	41.9	45	-44.1	-45	309.7	315	-234.9	-225	127.9	135
Port 8	-202	-202.5	334.8	337.5	-468.8	-472.5	67.2	67.5	-67.2	-67.5	468.8	472.5	-334.8	-337.5	202	202.5
PPD		-67.5		112.5		-157.5		22.5		-22.5		157.5		-112.5		67.5

be identical and equal to −6 dB. These figures show that the equal power for all ports with the error of 1.5 dB has been achieved and all S-parameters are above −7.8 dB in the Wi-Fi frequency band (2.4–2.5 GHz), which give a reasonable sidelobe level. For better comparison, the numerical values of Fig. 11 at the center frequency (2.45 GHz), are summarized in Table III. Moreover, the return loss values of all input ports are better than 20 dB over the bandwidth.

Table IV compares the simulated and measured normalized output phases for excitation from each input port. According to Tables III and IV, balanced insertion loss values and the appropriate PPDs have been achieved with average errors less than 7% and 5% from the ideal ones, respectively. The ideal value for insertion loss is 6.6 dB by assuming 0.6 dB loss for the structure. The measured 10 dB impedance bandwidth of the structure ranges from 2.2 to 2.8 GHz, which is 24%, while the size of the structure is about $1.8\lambda_0 \times 1.15\lambda_0$ at the center frequency of 2.45 GHz.

As it was mentioned, the proper PPDs of the first group of Table II is accomplished, so it is possible to reconstruct the similar radiated pattern of the 8 × 8 Butler matrix by employing two asymmetrical 4 × 4 Butler matrix of Fig. 10 beside each other in a single layer PCB configuration. The good agreement between simulation and measurement results demonstrates the robustness of the proposed design procedure.

B. Switched Version of the Asymmetrical 8 × 8 Butler Matrix

The structure proposed in Fig. 8 has been fabricated using the achieved values of the double asymmetrical 8 × 8 Butler matrix, which were mentioned in Fig. 10, with some modifications on the constant phase shifts (φ_1 to φ_4) to compensate for the extra lines added for the switches. The fabricated switched Butler array is shown in Fig. 12(a). The substrate is the same as the previous structure (RO 4003). AS193-000 IC was used in this circuit for SPDT switch. Fig. 12(b) displays the control board designed to control RF SPDT switches, including a microcontroller (Atmega32), and switch mode control button. The evaluation board designed to extract the properties of the switch is shown in Fig. 13(a). The measured S-parameters are shown in Fig. 13(b). The phase lag added by the switch compared to a straight line is 59°, which is compensated in the design. Thus, extra phase shift sections with the phase lag equal to that of the two switches (118°) are added to the paths of crossovers.

The measured S-parameters of the Butler Matrix are shown in Fig. 14. Similar to Fig. 11, the eight left plots show S_{ij}, where $i = 5$ to 8 and $j = 1$ to 4. Fig. 14 shows that the values of insertion loss for all ports and switch states are better than 11 dB in the Wi-Fi frequency band, and each insertion loss is nearly flat. The two right plots show the return loss of the structure for all ports, which is better than 15 dB in the desired frequency band. The numerical results of the insertion loss, as well as the normalized output phases at the center frequency, are shown in Tables V and VI, where mode (A) and mode (B) denote the state of the switches as it is depicted in Fig. 8. Mode (A) employs the first group phase shifts, which are described in Table II, and Mode (B) selects the second group.

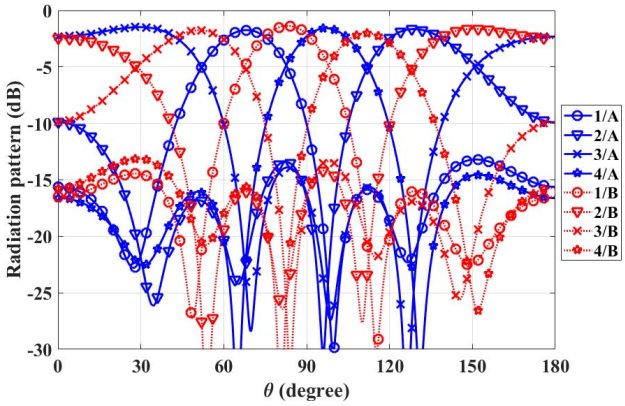

Fig. 15. Radiated pattern of the switched version of asymmetrical 8 × 8 Butler matrix by using measured values, considering isotropic antenna elements with half-wavelength spacing. (N/A or B: input number/switches state).

Table V shows that the average insertion loss is 1.8 dB, which is about 2 dB better than the 8 × 8 Butler matrix proposed in [16]. As anticipated, the loss of this structure is more than the first one because of some paths, which start from input to output, contain four SPDT switches with an average insertion loss of $4 \times 0.35 = 1.4$ dB according to Fig. 13(b). The unbalanced output power is the result of the fact that some signal paths from input to output, pass through four switches (e.g., S_{51},) while some other paths experience 2 switches (e.g., S_{82}) and the remaining paths do not encounter any switch in their ways (e.g., S_{73}).

The proper output phases shown in Table VI imply that the average error is less than 8%. The last row shows that the PPDs of 8 × 8 Butler matrix are accomplished by the switched version of asymmetrical 4 × 4 Butler matrix, which verifies the accuracy of the proposed design method.

Using the measured values of Tables V and VI and assuming isotropic pattern for antenna elements, the radiated pattern of

the switched version of the asymmetrical 8 × 8 Butler matrix is plotted in Fig. 15. As it is indicated, the maximum ripple of the gain (difference value of maximum gain and the lowest cross of the neighbor beams) is near 1.2 dB while sidelobe level for all main beams is better than 11.5 dB. According to Fig. 14, the 10 dB impedance bandwidth of the structure is from 2.06 to 2.56 GHz (20%). Also, the size of the structure is about $2.8\lambda_0 \times 1.4\lambda_0$ at the center frequency (2.45 GHz).

V. Conclusion

In this paper, a modified structure for 4 × 4 Butler matrix was proposed, which uses four constant phase shift sections. These phase shifts provide more degrees of freedom to design a flexible PPD at the outputs. By choosing proper values for these phase shifts, four beam patterns of the conventional 4 × 4 Butler matrix rotate around their main angle without degrading the gain of the main beam. Thus, this structure is called asymmetric Butler matrix. Consequently, the broadside direction or endfire direction can be covered. Using the proposed design approach two configurations were proposed to generate eight main beams similar to the 8 × 8 Butler matrix, which can be fabricated in a single layer PCB. These configurations were fabricated and measured for 2.45 GHz band. The measured insertion loss and phase imbalance are significantly lower than the conventional 8 × 8 Butler matrix. Furthermore, the size can be reduced up to 80%.

References

[1] J. Butler and R. Lowe, "Beam-forming matrix simplifies design of electronically scanned antennas," *Electron. Des.*, pp. 170–173, Apr. 1961.

[2] N. Jamaly, A. Derneryd, and Y. Rahmat-Samii, "Spatial diversity performance of multiport antennas in the presence of a butler network," *IEEE Trans. Antennas Propag.*, vol. 61, no. 11, pp. 5697–5705, Nov. 2013.

[3] T. Djerafi and K. Wu, "A low-cost wideband 77-GHz planar Butler matrix in SIW technology," *IEEE Trans. Antennas Propag.*, vol. 60, no. 10, pp. 4949–4954, Oct. 2012.

[4] C.-H. Tseng, C.-J. Chen, and T.-H. Chu, "A low-cost 60-GHz switched-beam patch antenna array with Butler matrix network," *IEEE Antennas Wireless Propag. Lett.*, vol. 7, pp. 432–435, 2008.

[5] A. A. M. Ali, N. J. G. Fonseca, F. Coccetti, and H. Aubert, "Design and implementation of two-layer compact wideband butler matrices in SIW technology for Ku-band applications," *IEEE Trans. Antennas Propag.*, vol. 59, no. 2, pp. 503–512, Feb. 2011.

[6] T. Zak and K. Sachse, "An integrated Butler matrix in multi-layer technology for multi-port amplifier applications," in *Proc. 14th Int. Conf. Microw., Radar Wireless Commun. (MIKON)*, vol. 1, May 2002, pp. 59–62.

[7] A. Grau, J. Romeu, S. Blanch, L. Jofre, and F. De Flaviis, "Optimization of linear multielement antennas for selection combining by means of a butler matrix in different MIMO environments," *IEEE Trans. Antennas Propag.*, vol. 54, no. 11, pp. 3251–3264, Nov. 2006.

[8] C.-C. Chang, R.-H. Lee, and T.-Y. Shih, "Design of a beam switching/steering Butler matrix for phased array system," *IEEE Trans. Antennas Propag.*, vol. 58, no. 2, pp. 367–374, Feb. 2010.

[9] K. Wincza, K. Staszek, and S. Gruszczynski, "Broadband multibeam antenna arrays fed by frequency-dependent Butler matrices," *IEEE Trans. Antennas Propag.*, vol. 65, no. 9, pp. 4539–4547, Sep. 2017.

[10] C.-W. Wang, T.-G. Ma, and C.-F. Yang, "A new planar artificial transmission line and its applications to a miniaturized Butler matrix," *IEEE Trans. Microw. Theory Techn.*, vol. 55, no. 12, pp. 2792–2801, Dec. 2007.

[11] Y. S. Jeong and T. W. Kim, "Design and analysis of swapped port coupler and its application in a miniaturized Butler matrix," *IEEE Trans. Microw. Theory Techn.*, vol. 58, no. 4, pp. 764–770, Apr. 2010.

[12] S. Gruszczynski and K. Wincza, "Broadband 4×4 butler matrices as a connection of symmetrical multisection coupled-line 3-dB directional couplers and phase correction networks," *IEEE Trans. Microw. Theory Techn.*, vol. 57, no. 1, pp. 1–9, Jan. 2009.

[13] K. Tekkouk, J. Hirokawa, R. Sauleau, M. Ettorre, M. Sano, and M. Ando, "Dual-layer ridged waveguide slot array fed by a butler matrix with sidelobe control in the 60-GHz band," *IEEE Trans. Antennas Propag.*, vol. 63, no. 9, pp. 3857–3867, Sep. 2015.

[14] J. Shelton, "Reduced sidelobes for Butler-matrix-fed linear arrays," *IEEE Trans. Antennas Propag.*, vol. AP-17, no. 5, pp. 645–647, Sep. 1969.

[15] G. Tudosie, R. Vahldieck, and A. Lu, "A novel modularized folded highly compact LTCC Butler matrix," in *IEEE MTT-S Int. Microw. Symp. Dig.*, Jun. 2008, pp. 691–694.

[16] B. Cetinoneri, Y. A. Atesal, and G. M. Rebeiz, "An 8×8 butler matrix in 0.13-μmCMOS for 5–6-GHz multibeam applications," *IEEE Trans. Microw. Theory Techn.*, vol. 59, no. 2, pp. 295–301, Feb. 2011.

[17] H. Ren, B. Arigong, M. Zhou, J. Ding, and H. Zhang, "A novel design of 4 × 4 Butler matrix with relatively flexible phase differences," *IEEE Antennas Wireless Propag. Lett.*, vol. 15, pp. 1277–1280, 2016.

[18] H. N. Chu and T.-G. Ma, "An extended 4 × 4 Butler matrix with enhanced beam controllability and widened spatial coverage," *IEEE Trans. Microw. Theory Techn.*, vol. 66, no. 3, pp. 1301–1311, Mar. 2018.

[19] A. B. Constantine *et al.*, "Antenna theory: Analysis and design," in *Microstrip Antennas*, 3rd ed. Hoboken, NJ, USA: Wiley, 2005.

[20] A. Tajik, M. Fakharzadeh, and K. Mehrany, "DC to 40-GHz compact single-layer crossover," *IEEE Microw. Wireless Compon. Lett.*, vol. 28, no. 8, pp. 642–644, Aug. 2018.

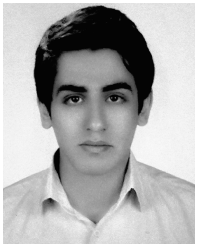

Ali Tajik received the B.S. degree in electrical engineering from the University of Tehran, Tehran, Iran, in 2015, and the M.S. degree in communication, fields and waves engineering from the Sharif University of Technology, Tehran, in 2018.

From 2013 to 2015, he was with the Microwave Group, University of Tehran, where he was involved in wireless power transfer using waveguide resonators. His current research interests include design and implementation of active and passive RF, microwave and millimeter-wave components as well as switched beam, and frequency beam scanning array antennas.

Ahmad Shafiei Alavijeh received the B.S. degree in electronic engineer from the M.A. University of Technology, Isfahan, Iran, in 2014, and the M.S. degree in electrical engineering from the Sharif University of Technology, Tehran, Iran, in 2017.

From 2014 to 2015, he was an Electronic Engineer with Rozhanco, Isfahan. From 2016 to 2019, he was an RF Engineer with the Sharif Millimeter-Wave Imaging Group, Tehran. His current research interests include RF active and passive circuits, the hardware design of transceivers, and the hardware optimizing of a millimeter-wave body scanner.

Mohammad Fakharzadeh (S'01–M'10–SM'12) received the M.Sc. degree in electrical engineering from the Sharif University of Technology, Tehran, Iran, in 2002, and the Ph.D. degree (Hons.) in electrical and computer engineering from the University of Waterloo, Waterloo, ON, Canada, in 2008.

He was the Manager of the antenna and packaging group with Peraso Technologies, Toronto, ON, Canada, where he was involved in developing the integrated millimeter-wave solutions for portable electronic devices and small-cell backhaul. He is currently an Associate Professor with the electrical engineering Department, Sharif University of Technology. He has over 18 years of experience in the design and implementation of phased-array antenna and mm-wave systems, particularly novel antenna and packaging solutions. He has authored more than 80 IEEE papers. He holds ten U.S. patents.